

# Effect of External Magnetic Field on Critical Current for the Onset of Virtual Cathode Oscillations in Relativistic Electron Beams

Alexander Hramov<sup>a</sup>, Alexey Koronovskii<sup>a</sup>, Mikhail Morozov<sup>a</sup>,  
Alexander Mushtakov<sup>a</sup>

<sup>a</sup>*Faculty of Nonlinear Processes, Saratov State University, Astrakhanskaya, 83,  
Saratov, 410012, Russia*

---

## Abstract

In this Letter we research the space charge limiting current value at which the oscillating virtual cathode is formed in the relativistic electron beam as a function of the external magnetic field guiding the beam electrons. It is shown that the space charge limiting (critical) current decreases with growth of the external magnetic field, and that there is an optimal induction value of the magnetic field at which the critical current for the onset of virtual cathode oscillations in the electron beam is minimum. For the strong external magnetic field the space charge limiting current corresponds to the analytical relation derived under the assumption that the motion of the electron beam is one-dimensional [High Power Microwave Sources. Artech House Microwave Library, 1987. Chapter 13]. Such behavior is explained by the characteristic features of the dynamics of electron space charge in the longitudinal and radial directions in the drift space at the different external magnetic fields.

*Key words:* plasma physics, electron beam, microwave high-power electronics, virtual cathode, vircator

---

## 1 Introduction

Beams of charged particles have great importance for understanding physical properties of plasmas, as well as for their technological applications. High power relativistic electron beams are used in plasma heating, inertial fusion, high-power microwave generation, and other. One of the most important directions of research in the high-power vacuum and plasma electronics is the study of the virtual cathode oscillators (vircators). The vircator is a microwave generator whose operation is based on oscillations of the virtual cathode (VC) in the electron beam with the overcritical current [1–3]. In recent years vircators have been widely studied experimentally [3–10], by computer simulation [3, 11–17] and analytical analysis [18–21]. Microwave radiation in vircators is generated when the current of a charged particle beam exceeds the critical (so-called space charge limiting) current  $I_{SCL}$  [1, 2]. Therefore, in order to understand the physical processes occurring in beams with the VC, it is important to determine the critical current  $I_{SCL}$  for the formation of the oscillating VC in the electron beam.

The problem of the limiting current for a beam injected into a diode gap was first treated in works of Child and Langmuir [22–24]. This problem was later considered by Pierce [25], who considered one-dimensional dynamics of the electron beam in the planar diode gap with a fixed neutralizing background (the so-called Pierce diode) and stated that the increase of the beam current

---

*Email address:* `aeh@nonlin.sgu.ru` (Alexander Hramov).

in Pierce diode can lead to instability (which came to be called the Pierce instability [26–29]) with the resulting formation of the VC [1]. Further studies presented that the development of the Pierce instability in the diode gap is accompanied by the various nonlinear oscillatory phenomena, such as chaotic spatiotemporal oscillations and the formation of coherent structures (see, for example, [26, 30–32]). Let us note, that the studies by Child and Langmuir were later generalized numerically to beams and drift spaces having a more complicated geometry [33].

Detailed analysis of the critical current values of relativistic electron beams with different geometries was given firstly by Bogdankevich and Rukhadze [18]. The work of Genoni and Proctor [19] produces later a more accurate relation for space charge limiting current (see also [1]). These results were obtained under the assumption that the motion of the electron beam is one-dimensional (or similarly, that the guiding electrons external magnetic field is infinitely strong). The theoretical condition for the space charge limiting current assuming one-dimensional electron motion is [1, 2, 18, 19]

$$I_{SCL} = \frac{mc^3}{e} \frac{(\gamma_0^{2/3} - 1)^{3/2}}{1 + 2 \ln(R/r_b)}, \quad \gamma_0 = \frac{1}{\sqrt{1 - (v_0/c)^2}}, \quad (1)$$

where  $R$  is the drift tube radius,  $r_b$  is the radius of solid beam,  $\gamma_0$  is the value of relativistic factor at injection in the drift space,  $v_0$  is the electron velocity at injection in drift space,  $c$  is the light speed,  $e$  is the electron charge, and  $m$  is the electron rest mass.

Nevertheless, the problem of how the critical current for the onset of the VC in the electron beam depends on the external axial magnetic field has been not completely studied. It appears therefore worthwhile to examine this

issue in order to gain clearer and deeper insight into the physical processes occurring in charged particle beams with the VC. It should be noted that in Refs. [14, 17, 34] the complex nonlinear dynamics of the electron beams with the VC in the finite external magnetic field was studied, but in those papers the problem of the dependence of the critical current for the onset of the VC oscillations on the parameters of the system, was not analyzed.

In the present Letter we report the results of numerical studies of how the critical current  $I_{SCL}$  for the formation of the unsteady oscillating VC in the weakly relativistic electron beam depends on the external axial magnetic field.

The Letter is organized as follows. In Section 2 the mathematical model of studied electron-beam system is briefly discussed. In Section 3 the results of investigations of how the external magnetic field affects the critical current at which the VC oscillations arises in the electron beam are presented. In Section 4 we discuss the physical processes that accompany the formation of the VC in the electron beam and govern the dependence  $I_{SCL}(B)$  described in Section 3 for different values of the external magnetic field. In conclusion, we summarize the main results discussed in our Letter.

## 2 General Formalism

The simulation model will be briefly described in this section. The drift space for the electron beam is the closed finite-length cylindrical waveguide region of length  $L$  and radius  $R$  with grid electrodes at both ends. An axially-symmetrical monoenergetic solid electron beam with the current  $I$  and radius  $R_b$  is injected at the velocity  $v_0$  through the left (entrance) grid and than

can be extracted through the right (exit) grid or escapes to the side wall of the drift tube. An external uniform guiding electrons magnetic field with induction  $B$  is applied along the waveguide axis.

We consider a time-dependent 2.5D model in which the dynamics of the electron beam in the drift space is described by solving a self-consistent set of Vlasov and Poisson equations [35,36]. The Vlasov kinetic equation for electron beam motion analysis is solved numerically by the particle method [35,37,38]. The potential distribution in the drift waveguide can thus be easily obtained by numerical solving the Poisson's equation in cylindrical geometry [35].

The model used in our study does not provide a correct analysis of the problem of the critical current of electron beams with the normalized velocity of  $\beta_0 = v_0/c \gtrsim 0.5$ , because it does not take into account the self-magnetic field of the electron beam and the associated beam pinching effects. Therefore we restrict ourselves to studying the critical currents of weakly relativistic electron beams.

The equations describing the dynamics of the weakly relativistic electron beam are formulated in terms of the following dimensionless variables of the potential  $\phi$ , the space charge field  $E$ , the electron density  $\rho$ , the electron velocity  $v$ , the spatial coordinates  $z$  and  $r$ , and the time  $t$ :

$$\begin{aligned} \varphi' &= (v_0^2/\eta_0) \varphi, & E' &= (v_0^2/L\eta_0) E, & B' &= (v_0/L\eta_0) B, & \rho' &= \rho_0 \rho, \\ v' &= v_0 v, & z' &= Lz, & r' &= Lr, & t' &= (L/v_0) t, \end{aligned} \tag{2}$$

Here the prime means the dimensionless values,  $\eta_0$  is the specific charge of electron,  $v_0$  and  $\rho_0$  are the velocity and space charge density of the electron beam at the entrance to the system, respectively, and  $L$  is the length of the

interaction space.

As mentioned above, unsteady processes in the electron beam injected into the drift space were simulated numerically by the particle method. In cylindrical geometry particles have the form of a charged ring. For each of those charged particles the equations of motion were solved with allowance for the weakly relativistic velocity of the beam electrons. In terms of dimensionless values (2), the equations of motion in cylindrical coordinates are written as

$$\frac{d^2 r_i}{dt^2} - r_i \left( \frac{d\theta_i}{dt} \right)^2 = \eta(z_i, \theta_i, r_i) \left( E_r + r_i B \frac{d\theta_i}{dt} \right), \quad (3)$$

$$r_i \frac{d^2 \theta_i}{dt^2} + 2 \frac{d\theta_i}{dt} \frac{dr_i}{dt} = -\eta(z_i, \theta_i, r_i) B \frac{dr_i}{dt}, \quad (4)$$

$$\frac{d^2 z_i}{dt^2} = \eta(z_i, \theta_i, r_i) E_z, \quad i = 1, \dots, N_0, \quad (5)$$

where

$$\eta(z_i, \theta_i, r_i) = \left( 1 - \frac{\beta_0^2}{2} \left[ \left( \frac{dr_i}{dt} \right)^2 + \left( r_i \frac{d\theta_i}{dt} \right)^2 + \left( \frac{dz_i}{dt} \right)^2 \right] \right). \quad (6)$$

Here,  $z_i$ ,  $r_i$ , and  $\theta_i$  are the longitudinal, radial, and azimuthal coordinates of the charged particles, respectively,  $E_z$  and  $E_r$  are the longitudinal and radial electric field components, respectively,  $B = B_z$  is the longitudinal component of the external magnetic field, whose radial component is assumed to be zero  $B_r = 0$ ,  $\beta_0 = v_0/c$ , where  $v_0$  is the electron beam velocity at the entrance to the system and  $c$  is the light speed. The fields do not have azimuthal components because the system is axially-symmetric. The subscript  $i$  denotes the number of particles and  $N_0$  is the full number of particles used to model the charged particles beam.

The potential distribution in the interaction space was calculated self-consistently

from Poisson's equation

$$\frac{1}{r} \frac{d\varphi}{dr} + \frac{d^2\varphi}{dr^2} + \frac{d\varphi^2}{dz^2} = \alpha^2 \rho, \quad (7)$$

where

$$\alpha = L \left( \frac{|\rho_0|}{\varphi_0 \varepsilon_0} \right)^{1/2} = \sqrt{2} \omega_p L / v_0 \quad (8)$$

is the dimensionless control parameter which depends on the beam current as  $\alpha \sim \sqrt{I}$  and is proportional to the length of the drift tube space as  $\alpha \sim L$ . Poisson's equation (7) was solved with the boundary conditions

$$\varphi(z=0, r) = 0, \quad \varphi(z=1, r) = 0, \quad \varphi(z, r=R) = 0, \quad (9)$$

$$\left. \frac{d\varphi}{dr} \right|_{r=0} = 0. \quad (10)$$

Condition (9) implies that drift region bounded by the conducting cylindrical surface of the radius  $R$  held at a zero potential. Condition (10) means that the radial electric field at the symmetry axis  $r=0$  is zero due to the axial symmetry of the interaction space.

For each particle, equations of motion (3)–(5) were integrated numerically by the second-order leap-frog method [35]. At each time step Poisson's equation (7) was solved on the two-dimensional mesh in cylindrical coordinates. In order to reduce the mesh noise, the space charge density on the mesh was calculated using a bi-linear weighing procedure for particles (the particle-in-cell (PIC) method) [35].

### 3 Critical current dependence on the external magnetic field

Let us consider the results of numerical study of how the external magnetic field affects the space charge limiting current  $I_{SCL}$  at which the VC oscillations arises. The value of the critical current is determined by the calculation of the trajectory of the charged particles in the phase space  $(\mathbf{r}, \mathbf{v})$ , where  $\mathbf{r}$  is a radius-vector and  $\mathbf{v}$  is a velocity of the charged particle. The moment when virtual cathode appears corresponds to reflection of a part of the electron beam backwards to the injection plane  $z = 0$ . In this case, appearance of the charged particles with negative longitudinal components of velocity ( $v_z < 0$ ) takes place. Onset of the oscillations of the virtual cathode is investigated by the analysis of the dynamics of the space charge electric field (both longitudinal  $E_z$ , and radial  $E_r$  components) in the drift space. The moment of appearance of charged particles reflections in the beam (virtual cathode formation) corresponds to the moment of onset of the electric field oscillations in the system. Let us note that if an injected current exceeds the critical current value insignificantly then the duration of the time interval required for virtual cathode formation and the reflected particle occurrence grows considerably (see [5]). Therefore we took into account this fact in the numerical simulation by means of choice of the duration of the numerical simulation large enough for the beam current being close to the value of the critical current. So, in this case the duration of the simulation exceeded  $200T_p$ , where  $T_p = 2\pi/\omega_p$  is the typical time scale,  $\omega_p$  is the plasma frequency of the electron beam. This duration corresponds approximately 100 periods of the virtual cathode oscillations.

We begin by analyzing the case in which the ratio of the initial beam radius



$r_b$  at the entrance to the interaction space to the radius  $R$  of the interaction space itself  $\sigma = r_b/R$  is fixed. We call  $\sigma$  the filling parameter, i.e. the parameter that characterizes the extent to which the drift space is filled with the electron beam. If it is not stipulated especially, the ratio of the drift tube radius to its length is assumed to be constant and is equal to  $R/L = 0.25$ . Fig. 1 shows how the normalized critical beam current  $I_{SCL}$  depends on the external magnetic field  $B$  for  $\sigma = 0.5$ . The critical beam current is normalized to its magnitude  $I_{SCL}$  at a zero external magnetic field ( $B = 0$ ). In Fig. 1 different curves correspond to different initial velocities  $\beta_0 = v_0/c$  of the electron beam injected into the drift tube. We can see that the dependence  $I_{SCL}(B)$  behaves differently in two characteristic ranges of the magnetic field  $B$ . At weak magnetic fields the critical beam current decreases monotonically as the external magnetic field  $B$  increases. At strong external magnetic fields the critical current of the electron beam increases monotonically with magnetic induction. Consequently, there is a certain magnetic field  $B_{\min}$  at which the critical beam

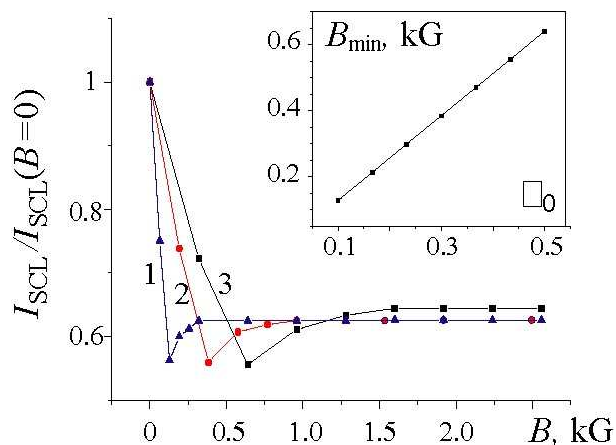


Fig. 1. Normalized critical (space charge limiting) current  $I_{SCL}/I_{SCL}(B = 0)$  vs external magnetic field  $B$  for  $\sigma = 0.5$  and for the different electron beam velocities: (1)  $\beta_0 = 0.1$ , (2) 0.3, and (3) 0.5. In the frame the optimum external magnetic field  $B_{\min}$  vs normalized electron velocity  $\beta_0$  is shown.

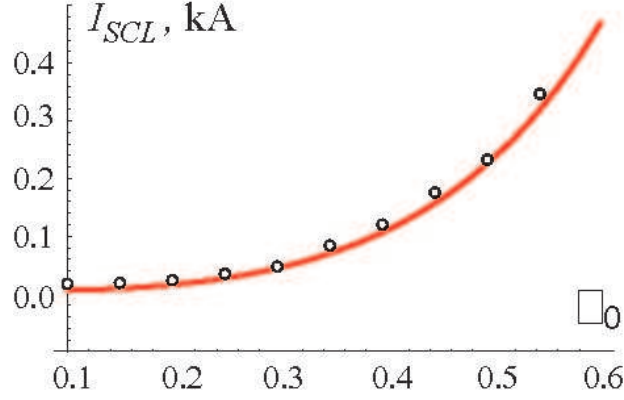


Fig. 2. Critical (space charge limiting) current  $I_{SCL}$  [kA] vs normalized electron beam velocity  $\beta_0$  for  $\sigma = 0.5$  and strong magnetic field  $B = 2.5$  kG (points  $\circ$ ). The solid line corresponds to the analytical relation (1) of the space charge limiting current.

current is minimum. This result is quite important because it provides the way to determine the optimum magnetic field for the onset of microwave generation in the virtual cathode oscillator at the minimum current of relativistic electron beam. Note, that at strong magnetic fields the critical beam current increases and asymptotically approaches to the analytical relation (1) of space charge limiting current which was obtained for an infinitely strong external magnetic field (and, as consequence, one-dimensional motion of the electron flow) [1]. For verification of the results of our simulation in Fig. 2 the analytical (Eq. (1)) and numerical dependencies of the critical current  $I_{SCL}$  on the normalized electron beam velocity  $\beta_0$  for strong magnetic field  $B = 2.5$  kG are shown. Comparison of the presented dependencies shows good agreement of the known analytical results and our numerical calculations.

The dependencies shown in Fig. 1 were calculated for different values of the electron beam velocity  $\beta_0$  at the entrance to the drift tube. We can see from Fig. 1, that for the non-relativistic and relativistic electron beams under con-

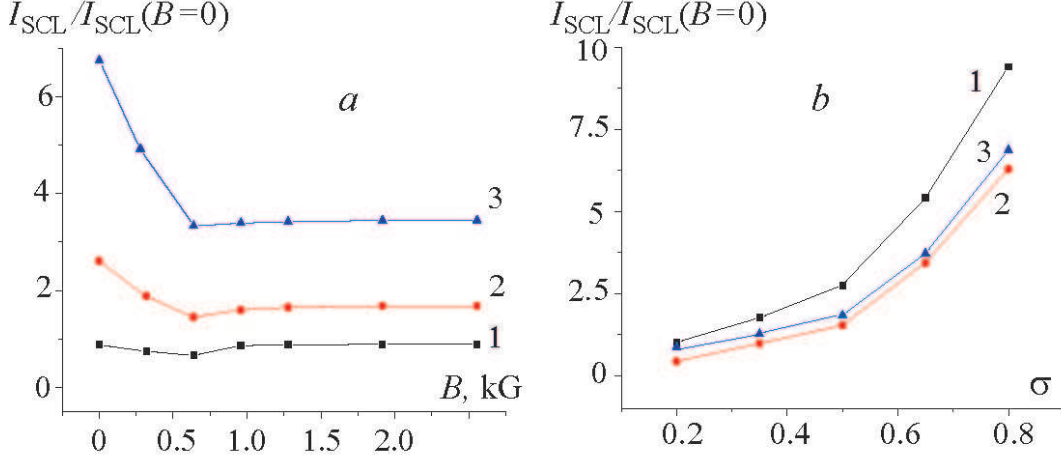


Fig. 3. (a) Normalized critical electron beam current  $I_{SCL}/I_{SCL}(B = 0)$  vs external magnetic field for different values of the filling parameter  $\sigma$  (the extent to which the drift tube is filled with the beam). Curve 1 corresponds to  $\sigma = 0.2$ , 2 – 0.5, and 3 – 0.9. (b) Normalized critical current vs. filling parameter  $\sigma$  for different inductions of the external magnetic field: (1)  $B = 0$ , (2)  $B = B_{\min} = 0.6$  kG, and (3)  $B = 2.5$  kG. The electron beam velocity at the entrance to the drift tube is such that  $\beta_0 = 0.5$

sideration here the dependence of the critical beam current  $I_{SCL}$  on the external magnetic field  $B$  is qualitatively the same for different beam velocities. For any velocity of the injected beam the critical current decreases with increasing  $B$  in the range of the weak external magnetic fields, and, otherwise, it increases monotonically in the range of the strong magnetic fields. However, the optimal magnetic field  $B_{\min}$  depends on the electron beam velocity  $\beta_0$ . The dependence of  $B_{\min}$  on  $\beta_0$  is shown in the frame in Fig. 1 from which we can see that the optimum external magnetic field increases linearly with the velocity  $\beta_0$  of the injected electron beam.

Let us now consider the dependence of the critical current for the formation of the VC oscillation on the external magnetic field for different values of the filling parameter  $\sigma$  and the ratio  $R/L$  of the drift tube radius to its length.

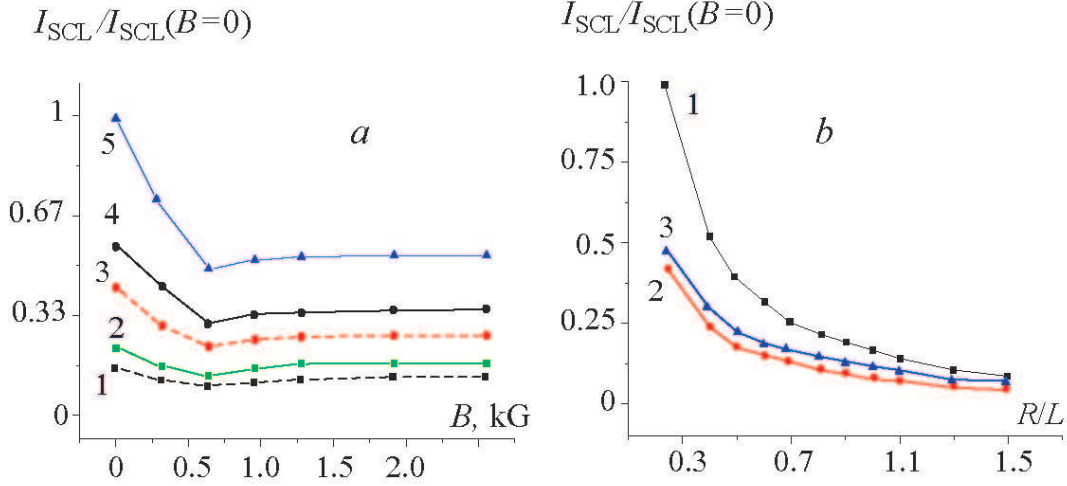


Fig. 4. (a) Normalized critical electron beam current  $I_{SCL}/I_{SCL}(B = 0)$  vs external magnetic field for different values of the ratio of the drift tube radius to its length for fixed beam radius  $r_b/L = 0.25$ . Curve 1 corresponds to  $R/L = 1.3$ , 2 – 1.0, 3 – 0.5, 4 – 0.4, and 5 – 0.3. (b) Normalized critical current vs. the ratio  $R/L$  for different inductions of the external magnetic field: (1)  $B = 0$ , (2)  $B = B_{\min} = 0.6$  kG, and (3)  $B = 2.5$  kG. The electron beam velocity at the entrance to the drift tube is such that  $\beta_0 = 0.5$

Fig. 3(a) presents the corresponding dependencies  $I_{SCL}(B)$  for different  $\sigma$  values and for the fixed electron beam velocity  $\beta_0 = 0.5$  at the entrance to the drift tube. We can see, that the current required for the formation of the oscillating VC increases with the filling parameter. In Fig. 3(b) the critical beam current dependencies on the filling parameter  $\sigma$  for different values of the external magnetic field are shown. It can be seen that the critical beam current  $I_{SCL}$  increases monotonically with  $\sigma$ , and that for different external magnetic fields the dependence  $I_{SCL}(\sigma)$  remains essentially the same.

Fig. 4(a) shows the dependencies  $I_{SCL}(B)$  for different values the ratio  $R/L$  of the drift tube radius to its length and for the fixed electron beam velocity  $\beta_0 = 0.5$ . In this case the current required for the formation of the oscillating

VC decreases with the growth of the  $R/L$  value. In Fig. 3(b) the critical current dependencies on the geometry parameter  $\sigma$  for different values of the external magnetic field are shown. It can be seen that the critical beam current  $I_{SCL}$  decreases monotonically with  $R/L$ , and that for different external magnetic fields the dependence  $I_{SCL}(R)$  remains essentially the same.

It should be noted that the optimal magnetic field  $B_{\min}$ , at which the critical beam current is minimal, does not essentially depend on the filling parameter  $\sigma$  and geometry parameter  $R/L$  and is determined only by the velocity  $\beta_0$ . For different values of the parameters  $\sigma$  and  $R/L$  the critical beam current accepts minimal value for the optimal external magnetic field  $B = B_{\min}$  (see curves 2 in Figs. 3(b) and 4(b)).

#### **4 Physical processes in the electron beam with overcritical current at the external magnetic field**

Let us consider the physical processes that accompany the oscillating VC formation in the electron beam and govern the dependence  $I_{SCL}(B)$  described in previous Section 3 for different inductions  $B$  of the guiding magnetic field.

We begin by analyzing the dependence of the beam current distribution in the system on the external magnetic field. To do this, we consider how the numbers of large charged particles that escape from the drift space through its entrance and exit planes and through its side surface depending on the external magnetic field. Fig. 5 shows how the normalized numbers  $N$  of particles that are reflected from the VC and escape from the drift space through the entrance grid (curve 2 in Fig. 5) and through the side surface (curve 1) and that pass

through the VC and escape from the drift space through the exit grid (curve 3) depend on the axial magnetic field in the drift space. The calculations were carried out for the filling parameter  $\sigma = 0.5$  and for the beam velocity  $\beta_0 = 0.5$ .

From Fig. 5 we can see that the escape dynamics of the charged particles from the drift space differs radically in the cases of the weak and the strong values of the external magnetic field. In the case of the weak magnetic field  $B < 0.5$  kG, a large number of charged particles escape from the drift space through its side wall. The number of such particles, that are reflected from the VC and escape from the system in the radial (transverse) direction, is maximum at zero external magnetic field and decreases monotonically with magnetic induction increasing (see curve 1 in Fig. 5). At the same time, the number of particles that are reflected from the VC in the longitudinal direction and escape through the injection plane  $z = 0$ , as well as the number of particles that pass through the oscillating VC and escape from the drift space through the exit grid, increases with the external magnetic field (see Fig. 5, curves 2 and 3 respectively). In Fig. 1 such behavior of the number of charged particles that are reflected from the VC in the longitudinal and transverse directions corresponds to the range  $B < B_{\min}$  in which the critical beam current decreases with increasing external magnetic field (cf. the curves in the range  $B < 0.5$  kG in Fig. 1 versus the curves in the same range in Fig. 5).

For stronger magnetic fields,  $B > 0.5$  kG there are almost no charged particles that are reflected from the VC in the transverse direction and escape radially from the drift space through its side wall (see Fig. 5). The number of particles moving in the longitudinal direction and escaping from the drift space through the entrance and exit grids remains unchanged with the increasing of the

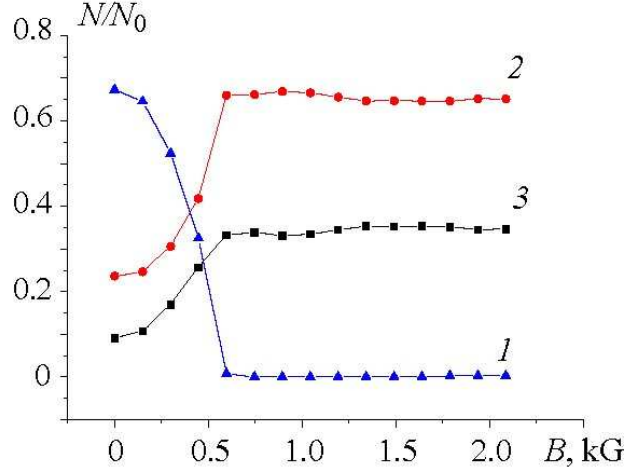


Fig. 5. (a) Normalized number  $N/N_0$  of charged particles escaping from the drift space through the side wall (curve 1) and through the entrance and exit grid electrodes (curves 2 and 3, respectively) versus external magnetic field for  $\beta_0 = 0.5$  and  $\sigma = 0.5$ . The value  $N_0$  is the total number of injected charged particles

external magnetic field (see Fig. 5, curves 2 and 3). A comparison between Figs. 1 and 5 shows that the magnetic field at which the transverse dynamics of the charged particles reflected from the VC becomes unimportant (i.e.  $N \approx 0$ ) and is close to the optimal magnetic field  $B_{\min}$  at which the critical space charge limiting current is minimum.

Such behavior of the electron beam allows us to suggest that at the weak external magnetic field the formation and dynamics of the VC oscillations differ from those at the strong magnetic field. In the weak magnetic field  $B < B_{\min}$ , which poorly confines the electrons, the transverse dynamics of the electron beam plays a predominant role in the drift space. For the strong external magnetic field that the current through the side surface bounding the drift tube in the radial direction is zero the longitudinal dynamics of the space charge of the beam is dominated in the analyzed system. Let us note that cyclotron rotation of electrons in the magnetic field is observed simultaneously.

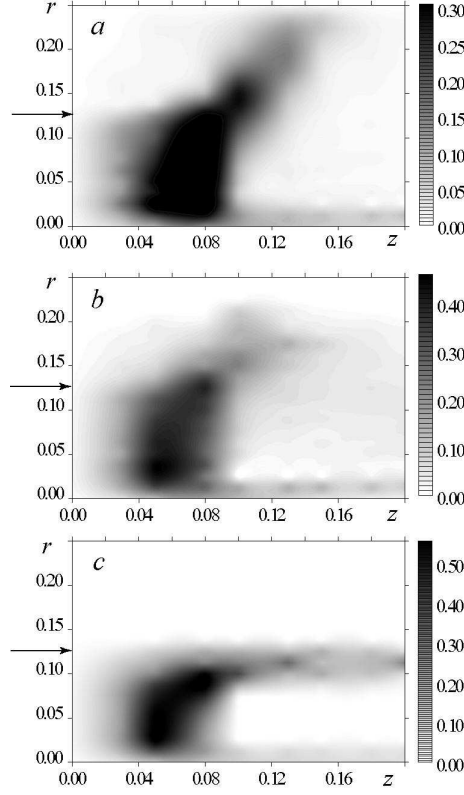


Fig. 6. Space charge density distributions in the VC region, averaged over the characteristic period of VC oscillations for the filling parameter  $\sigma = 0.5$  and different inductions of the external magnetic field: (a)  $B = 0$ , (b)  $B = B_{\min} = 0.6 \text{ kG}$ , and (c)  $B = 2.0 \text{ kG}$ . The arrows show the initial radial beam boundary. Longitudinal coordinate is shown on the abscissa and radial coordinate is shown on the ordinate. The gray color intensity is proportional to the absolute value of the space charge. The scale from the right side of the figure shows the values of the space charge density.

At the intermediate magnetic fields  $B \sim B_{\min}$  the behavior of the system is governed by both the transverse and longitudinal dynamics of the space charge in the VC region.

Let us examine in more detail the behavior of the electron beam in the VC area at different inductions of the external magnetic field. The space charge density distributions in the area of VC oscillations ( $z \in (0, 0.2)$ ) averaged



over the characteristic period of VC oscillations for different inductions  $B$  is shown in Figs. 6. In these figure the absolute values of the dimensionless space charge density  $|\rho(r, z)|$  at different points  $(r, z)$  in the drift space are shown by shades of gray. The maximum in the space charge density (the dark region in the distributions  $|\rho(r, z)|$ ) corresponds to the VC region, where the electrons are stopped and start moving back toward the injection plane or toward the side wall of the drift tube. The electron beam is decelerated by the space charge of the VC and the electron velocities within it are close to zero. So, the space charge density  $|\rho|$  achieves the maximum value in the VC region.

From the distributions shown in Figs. 6(a), which were calculated for the zero external magnetic field, we can see that in the VC region the electron beam greatly expands in the transverse (radial) direction, so the beam space charge density near the injection plane is nonzero over the entire cross transverse section of the drift tube. For the weak external magnetic field the space charge density distribution is qualitatively the same. This behavior of the electron beam can be explained as follows. A dense electron bunch formed in the VC region (and, accordingly, decelerates the electron beam) gives rise to fairly strong space charge forces (the Coulomb repulsion between the electrons), under the effect of which the electrons acquire the transverse velocity, rapidly escape in the radial direction, and are lost at the side cylindrical wall bounding the drift tube.

Such a transverse electron dynamics under the effect of space charge forces in the absence of the external magnetic field or in the weak external magnetic field, which does not restrain these forces, results in substantial radial expansion of the beam. As a consequence, in the weak external magnetic field most of the beam electrons in the VC region move in the transverse (radial) direc-

tion with respect to the drift tube axis. The radial beam expansion reduces the space charge density in the VC and, accordingly, increases the space charge limiting current  $I_{SCL}$  for achieving the space charge density required for the formation of the oscillating VC. In this case some of the electrons begin to be reflected to the entrance grid and are turned to the side surface of the drift tube.

As can be seen from Fig. 6(a), the electron bunch in the VC region extends over the entire transverse cross section of the drift tube. In this case, the space charge density is maximum ( $|\rho| > 0.25$  in dimensionless units) within the radial region whose radius exceeds the initial beam radius  $r_b$  (shown by the arrow in Fig. 6(b)). The radial region of maximum space charge density is displaced in the propagation direction of the injected electron beam. This indicates that the distribution  $\rho(r, z)$  in the VC region is nonuniform in both the radial and longitudinal directions.

For the small filling parameter  $\sigma$  the system behaves in the similar manner. In this case the lower critical current of electron beam is determined by the higher space charge density of the electron beam because of the smaller beam cross-sectional area for the fixed parameter  $\alpha$  which is proportional to the injected beam current  $I$ . Consequently, the space charge density level required for the formation of the VC oscillations in the beam of larger radius is achieved when the electron beam current is higher than that of the beam with smaller radius. This conclusion, which is confirmed by numerical simulations (see Fig. 3), is valid for an arbitrary induction  $B$  of the external magnetic field.

Let us note, that for the weak magnetic field the electron bunch in the VC region oscillates mainly in the radial direction. In this case the maximum space

charge density and the spatial position of the VC vary only slightly with time, in contrast to the case of strong external magnetic fields, in which the electron dynamics is essentially one-dimensional (see, e.g., [1,16,39]). Radial oscillations can occur with the lower beam space charge densities than those at which the VC can execute longitudinal oscillations.

A stronger magnetic field  $B$  prevents the beam electrons moving in the radial direction and imparts the azimuthal velocity to them. As a result, the number of electrons escaping from the drift space radially through the side wall of the system decreases as the magnetic induction  $B$  increases (see Fig. 5). Fig. 6(b) shows the averaging space charge density distributions in the VC region for the optimal magnetic field  $B = B_{\min}$ . It is possible to see that the external magnetic field restricts radial electron motion, increasing the space charge density in the VC region (cf. the gray scale on the right of Figs. 6(a) and 6(b)). Consequently, as follows from Fig. 1 decreasing the critical current at which the electrons begin to be reflected and the oscillating VC arises in the beam.

Fig. 6(c) shows that in the strong magnetic field such that the beam dynamics close to one-dimensional ( $B \gg B_{\min}$ ), the VC (the region of maximum space charge density) ranges almost entirely within the initial beam radius. The initial beam radius  $r_b$  is indicated by the arrow in Fig. 6. In this case radial oscillations of the space charge density are not observed. At strong magnetic fields the oscillatory behavior of the VC agrees well with the VC oscillations in the one-dimensional case described in detail in Refs. [21, 28, 31] for the 1D model of the electron beam with the VC. As consequence, VC oscillations behavior and the space charge limiting current weakly depends on the external magnetic field in the range  $B \gg B_{\min}$ .

Based on the fact that the space charge dynamics differs radically in the cases of the weak and the strong external magnetic field, we may speak of two different types of oscillating VC. In the weak magnetic field, the formation of the VC and its oscillations are governed primarily by the transverse dynamics of the beam electrons under the effect of the repulsive space-charge forces, which substantially expands the beam in the radial direction. In this case we may speak of the *transverse* VC in which the space charge density oscillates predominantly in the radial direction. The situation is radically different for the strong external magnetic fields when the longitudinal electron dynamics is dominated and the space charge density oscillates predominantly in the longitudinal direction. In this case we may speak of the *longitudinal* VC in an electron beam with an overcritical current. The behavior of such beams with the longitudinal VC oscillations has been studied in more detail by the numerical simulation [11–13, 15, 16]. Such oscillating regimes are typical of vircators operating with a strong external magnetic field [3, 15]. Accordingly, the critical beam current is described by the familiar relationship (1) [1].

At intermediate external magnetic fields  $B \sim B_{\min}$  competition between the longitudinal and transverse oscillations of the space charge density in the electron beam with the VC gives rise to the minimum in the dependence  $I_{SCL}(B)$  of the space charge limit current on the external magnetic field.

## 5 Conclusion

Thus, the influence of the external magnetic field on the space charge limiting current corresponding to the onset of the oscillating VC in the electron beam is reported for the first time in this Letter. It is shown that the critical current

decreases when external magnetic field increases. There is the optimal magnetic field at which the space charge limiting current is minimum. For stronger external magnetic fields the critical current is described by the familiar relation (1) [1] obtained under the assumption that the motion of the electrons is one-dimensional. Study of the physical processes in the electron beam with the virtual cathode presents that the dependence of the critical current on the external magnetic field is governed by the characteristic features of the longitudinal and radial dynamics of the electron space charge in the drift tube at different inductions of the axial magnetic field.

In the weak external magnetic field the major role is played by the transverse beam dynamics (i.e. the two-dimensional effects associated with the Coulomb repulsion of the electrons in the radial direction). As a consequence, the space charge density in the VC area reduces, so the oscillating VC can arise in the electron beam with the higher current in comparison with that at strong magnetic fields. When the external magnetic field is strong the transverse beam dynamics is less important and the behavior of the VC is governed primarily by the longitudinal oscillations in the electron beam.

## **Acknowledgments**

We thank Dr. S.V. Eremina for English language support. This work was supported by U.S. Civilian Research and Development Foundation for the Independent States of the Former Soviet Union (CRDF), grant REC-006, the Supporting program of leading Russian scientific schools (project NSh-4167.2006.2) and Doctor of Science (project MD-1884.2007.2), Russian Foundation of Basic Research (05-02-16286 and 06-02-81013) and “Dynasty” Foun-

dition.

## References

- [1] D. J. Sullivan, J. E. Walsh, E. Coutsias, Virtual cathode oscillator (vircator) theory, granatstein, v.l. and alexeff, i. Edition, Vol. 13 of High Power Microwave Sources, Artech House Microwave Library, 1987, p. 441.
- [2] D. I. Trubetskov, A. E. Hramov, Lectures on microwave electronics for physicists, Vol. 1,2. Fizmatlit, Moscow, 2003, 2004.
- [3] A. E. Dubinov, V. D. Selemir, Electronic devices with virtual cathodes (review), Journal of Communications Technology and Electronics 47 (6) (2002) 575.
- [4] H. Sze, D. Price, B. Harteneck, Phase locking of two strongly coupled vircators, J.Appl.Phys. 67 (5) (1990) 2278–2282.
- [5] V. D. Alyokhin, A. E. Dubinov, V. D. Selemir, O. A. Shamro, N. V. Stepanov, V. E. Vatrugin, Theoretical and experimental studies of virtual cathode microwave devices, IEEE Trans. Plasma Sci. 22 (5) (1994) 954.
- [6] H. Sze, J. Benford, L. T. Young, A radially and ill extracted virtual cathode oscillator (vircator), IEEE Trans. Plasma Sci. 15 (6) (1985) 592.
- [7] H. Sze, J. Benford, B. Harteneck, Dynamics of virtual cathode oscillator driven by pinched diode, Phys. Fluids 29 (11) (1986) 5875.
- [8] K. J. Hendricks, R. Adler, R. C. Noggle, Experimental results of phase locking two virtual cathode oscillators, J.Appl.Phys. 68 (2) (1990) 820–828.
- [9] H. A. Davis, R. R. Bartsch, T. J. Kwan, E. G. Sherwood, R. M. Stringfield, Experimental confirmation of the reditron concept, IEEE Trans. Plasma Sci. 16 (2) (1988) 192.

- [10] Y. Kalinin, A. A. Koronovskii, A. E. Hramov, E. N. Egorov, R. A. Filatov, Experimental and theoretical investigations of stochastic oscillatory phenomena in a nonrelativistic electron beam with a virtual cathode., Plasma Phys. Reports 31 (11) (2005) 938–952.
- [11] W. Jiang, H. Kitano, L. Huang, K. Masugata, K. Yatsui, Effect of longitudinal magnetic field on microwave efficiency of virtual cathode oscillator, IEEE Trans. Plasma Sci. 24 (1996) 187.
- [12] W. Jiang, K. Masugata, K. Yatsui, New configuration of a virtual cathode oscillator for microwave generation, Phys.Plasmas 2 (12) (1995) 4635.
- [13] T. J. Kwan, H. A. Davis, Numerical simulations of the reditron, IEEE Trans. Plasma Sci. 16 (2) (1988) 185–191.
- [14] X. Chen, W. K. Toh, P. A. Lindsay, Physics of the interaction process in a typical coaxial virtual cathode oscillator based on computer modelling using MAGIC, IEEE Trans. Plasma Sci. 32 (2004) 835.
- [15] T.-L. Lin, W.-T. Chen, W.-C. Liu, Y. Hu, Computer simulation of virtual cathode oscillations, J.Appl.Phys. 68 (5) (1990) 2038–2044.
- [16] V. G. Anfinogentov, A. E. Hramov, On the mechanism of occurrence of chaotic dynamics in a vacuum microwave generator with virtual cathode, Radiophysics and Quantum Electronics 41 (9) (1998) 1137.
- [17] E. N. Egorov, A. E. Hramov, Investigation of the chaotic dynamics of an electron beam with a virtual cathode in an external magnetic field, Plasma Physics Reports 32 (8) (2006) 683.
- [18] L. A. Bogdankevich, A. A. Rukhadze, Sov. Phys. Uspekhi 14 (1971) 163.
- [19] T. C. Genoni, W. A. Proctor, Upper bound for the space-charge limiting current of annular electron beams. J. Plasma Phys. 23 (1980) 129.

- [20] W. Woo, Two dimensional features of virtual cathode and microwave emission. Phys. Fluids 30 (1987) 239.
- [21] W. Jiang, K. Masugata, K. Yatsui, Mechanism of microwave generation by virtual cathode oscillation, Phys. Plasmas 2 (3) (1995) 982–986.
- [22] C. D. Child, Discharge from Hot CaO, Phys. Rev 32 (492).
- [23] I. Langmuir, K. B. Blodgett, Current limited by space charge between coaxial cylinders, Phys. Rev 22 (1923) 347.
- [24] I. Langmuir, K. B. Blodgett, Current limited by space charge between concentric spheres, Phys. Rev 23 (1924) 49.
- [25] J. R. Pierce, Limiting currents in electron beam in presence ions, J.Appl.Phys. 15 (1944) 721.
- [26] B. B. Godfrey, Oscillatory nonlinear electron flow in Pierce diode, Phys. Fluids 30 (1987) 1553.
- [27] W. S. Lawson, Phys. Fluids B (1989) 1493.
- [28] H. Matsumoto, H. Yokoyama, D. Summers, Computer simulations of the chaotic dynamics of the Pierce beam–plasma system, Phys.Plasmas 3 (1) (1996) 177.
- [29] R. A. Filatov, A. E. Hramov, A. A. Koronovskii, Chaotic synchronization in coupled spatially extended beam-plasma systems, Phys. Lett. A 358 (2006) 301–308.
- [30] T. Klinger, C. Schroder, D. Block, F. Greiner, A. Piel, G. Bonhomme, V. Naulin, Chaos control and taming of turbulence in plasma devices, Phys.Plasmas 8 (5) (2001) 1961–1968.
- [31] A. A. Koronovskii, A. E. Hramov, Wavelet bicoherence analysis as a method for investigating coherent structures in an electron beam with an overcritical current, Plasma Physics Reports 28 (8) (2002) 666.



- [32] A. E. Hramov, A. A. Koronovskii, I. S. Rempen, Controlling chaos in spatially extended beam-plasma system by the continuous delayed feedback, *Chaos* 16 (1) (2006) 013123.
- [33] J. W. Luginsland, Y. Y. Lau, R. M. Gilgenbach, Two-dimensional child-langmuir law, *Phys. Rev. Lett.* 77 (22) (1996) 4668–4670.
- [34] P. A. Lindsay, W. K. Toh, X. Chen, The influence of an axial magnetic field on the performance of a coaxial vircator, *IEEE Trans. Plasma Sci.* 30 (3) (2002) 1186–1195.
- [35] C. K. Birdsall, A. B. Langdon, *Plasma physics, via computer simulation*, NY: McGraw–Hill, 1985.
- [36] T. M. Anderson, A. A. Mondelli, B. Levush, J. P. Verboncoeur, C. K. Birdsall, Advances in modelling and simulation of vacuum electron devices, *Proceedings IEEE* 87 (5) (1999) 804–839.
- [37] D. Potter, *Computational physics*, John Wiley & Sons Ltd., 1973.
- [38] R. W. Hockney, J. W. Eastwood, *Computer simulation using particles*, NY: McGraw–Hill, 1981.
- [39] C. K. Birdsall, W. B. Bridges, *Electron dynamics of diode regions*, N. Y.: Academic Press, 1966.